RSC Advances

ROYAL SOCIETY OF CHEMISTRY

www.rsc.org/advances

Table of Contents

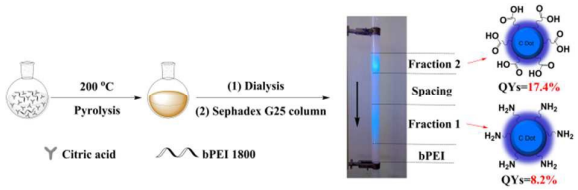

Highlight

Co-existence of carboxylic group-rich C-Dots and amine group-rich C-Dots during one-pot pyrolysis of citric acid and bPEI was firstly identified.

Journal Name

RSCPublishing

ARTICLE

Identifying the existence of highly-fluorescent carboxylic group-rich carbon nanodots during one-pot synthesis of branched polyethylenimine-passivated amine group-rich carbon nanodots

Cite this: DOI: 10.1039/xoxxoooooox

Received ooth January 2012,
Accepted ooth January 2012

DOI: 10.1039/xoxxoooooox

www.rsc.org/

Dan-Dan Liu,[a] Hua Su,[b] Qian Cao,[b] Xue-Yi Le*[a] and Zong-Wan Mao*[a, b]

Carbon nanodots (C-Dots) have been proposed as promising alternatives to traditional semiconductor quantum dots and organic fluorophores recently. However, C-Dots are often prepared and studied as a mixture, and the neglect of the real composition significantly limited the accurate understanding and control of physical/chemical properties of C-Dots and the further practical applications. Herein, we demonstrated and identified for the first time the co-existence of highly-fluorescent carboxylic group-rich C-Dots (CR-C-Dots) and amine group-rich C-Dots (AR-C-Dots) during one-pot pyrolysis of citric acid and bPEI precursors. Transmission electron microscopy demonstrated that the averaged size of CR-C-Dots was slightly smaller than that of amine group-rich C-Dots (AR-C-Dots), 1.5 nm vs 1.9 nm. Photophysical characterization indicated that CR-C-Dots had longer fluorescence lifetime and higher quantum yields (QYs) than AR-C-Dots, despite the same excitation-independent emission at 445 nm, different from most previous reports that amine group passivation enhanced QYs of C-Dots. Both C-Dots showed excellent biocompatibility and great potential for cellular imaging. A fluorescence- and electron spin resonance- responsive dual-model probe for ascorbic acid detection was also constructed, further proving the existence of CR-C-Dots. This study will facilitate the understanding of the nucleation/surface passivation process during C-Dots formation and development of new synthetic/purification strategy for C-Dots.

Introduction

As a new star in carbon materials family, fluorescent carbon nanodots (C-Dots) have attracted tremendous interests since the serendipitous discovery during purification of single walled carbon nanotubes by arc-discharge methods.[1] Owing to their significant advantages in resistance to photobleaching, good biocompatibility, easy preparation and rich surface functional groups for further modification,[2, 3] C-Dots have been applied in bioimaging,[4, 5] sensing,[6, 7] energy conversion,[8, 9] drug delivery,[10-12] and so on. In order to tune photophysical properties and structures of C-Dots, several physical or chemical strategies have been developed, which can be classified into top-down (arc-discharge,[1] laser-ablation,[13] electrochemical-oxidation,[14] *etc*.) and bottom-up strategy (pyrolytic methods,[15, 16] microwave methods,[17] hydrothermal methods,[18] *etc*.). Among these methodologies, bottom-up methods based on suitable molecular precursors and appropriate carbonization conditions have been demonstrated as an effective pathway to control the structure, size, morphology and photophysical properties of C-Dots.[15, 19, 20]

Despite the controversial nature of photoluminescence of C-Dots, surface passivation with nitrogen-containing organic molecules has been widely accepted as an effective strategy to tune the photophysical properties and functions of C-Dots (such as selective molecule/ion recognition).[21] Pioneering work by Sun *et al*.[13] demonstrated significantly enhanced fluorescence intensity of C-Dots upon surface passivation by diamine-

terminated polyethylene glycol. Zeng *et al*.[22] also controlled the emission profiles of C-Dots (excitation-dependent or independent) by simply changing the surface passivation degree of amine group. Notably, branched polyethylenimine (bPEI) was recently considered as promising passivation agents, due to their excellent abilities in surface trapping states control of C-Dots and unique metal ion/nucleic acid binding. For example, a one-pot carbonization and surface functionalization strategy has been demonstrated by Chi *et al*.[23, 24] recently to prepare highly luminescent and Cu^{2+}-responsive polyamine-functionalized C-Dots by pyrolysis of citric acid and branched polyethylenimine (bPEI). Liu *et al*.[25] also prepared highly luminescent bPEI-passivated C-Dots for DNA delivery based on one-pot microwave irradiation of glycerol and bPEI. It should be noted that only simple dialysis process for purification was conducted in most studies, neglecting the real composition of C-Dots produced in mysterious carbonization and passivation process. Is it true that amine-group passivated C-Dots are the solely formed species when preparing bPEI-passivated C-Dots?

It is well-known that the inhomogenous C-Dots might hinder the accurate understanding and control of physical/chemical properties and limit the further practical applications.[26] Apparently, co-existence of unpassivated C-Dots or free bPEI maybe lead to incorrect evaluation of the metal/nucleic acid binding or even cellular uptake of bPEI-passivated C-Dots. Therefore, it is significant to understand the confusing process during one-pot preparation of bPEI-passivated C-Dots. The possible mechanism of carbonization of citric acid and bPEI at low temperature has been proposed by Chi *et al*.: the initially completed carbonization of citric acid and formation of carbonaceous core at low temperature (< 200 ^{o}C) followed by the surface passivation of bPEI upon long-time heating.[24] This suggested that carboxylic group-rich C-Dots (CR-C-Dots) and amine group-rich C-Dots (AR-C-Dots) might simultaneously exist. However, identification and assignment of the existing species during this process is still challenging.

In the present work, highly-fluorescent CR-C-Dots and AR-C-Dots were simultaneously synthesized and identified for the first time during one-pot pyrolysis of citric acid and bPEI precursors. Separated by a simple Sephadex gel chromatography, two kinds of C-Dots with different surface properties and fluorescent profiles were obtained and further characterized in detail. A fluorescence and electron spin resonance-responsive dual-model probe for ascorbic acid was also constructed based on as-prepared CR-C-Dots, further proving the existence of CR-C-Dots. Preliminary biocompatibility test and cellular imaging study were also conducted.

Experimental

Reagents

Citric acid (CA, anhydrous, 99.5%) was purchased from Alfa Aesar. Branched polyethylenimine (bPEI, MW 1800 Da, 99%), 1-ethyl-3-(3-dimethylaminopropyl) carbodiimide hydrochloride (EDC, 98.5%) and N-hydroxysuccinimide (NHS, 98.5%) were purchased from Aladdin Reagent (Shanghai, China). 4-amino-2,2,6,6-tetramethylpiperidine 1-Oxyl free radical (4-AT, >97.0%) was bought from TCI Co., Ltd (Shanghai, China) and used as received. L-ascorbic acid (AA, 99%) was obtained from J&K Chemical Ltd (Beijing, China). The dialysis bag (molecular weight cutoff, MWCO 500-1000 Da) was obtained from Ebioeasy Corporation (Shanghai, China). Sephadex G-25 was purchased from GE Healthcare Bio-Science AB (Beijing, China) and used according to the manufacturer's instructions. $CuCl_2$, $FeCl_3$, ammonia water, NaOH and HCl were analytical grade and purchased from Guangzhou Chemical Reagent Factory. Ultra-pure water (18.2 MΩ) was used through the whole experiments.

Synthesis and separation of C-Dots

The C-Dots were synthesized by modifying the previously reported pyrolytic method.[23, 24] In the typical experiment, 1 g of citric acid and 0.5 g of bPEI were mixed uniformly with 10 mL water in a 25 mL three-necked beaker and heated up to 200 ^{o}C with a heating mantle in air. Once the yellow gel formed, 1 mL ultra-pure water was added. This process was repeated 10 times in 1 h before cooling down to room temperature. The resulting yellow gel was dissolved in 10 mL of ultra-pure water and dialysed against pure water for one day (MWCO 500-1000 Da). The obtained solution was then concentrated with rotary evaporator and passed through a GE Sephadex G25 chromatography (2.5 cm × 65 cm), eluted by 0.5% ammonia water for purification. Two kinds of C-Dots were obtained as yellow powders following lyophilization for further characterization and application.

Synthesis of C-Dots-4-AT

An aqueous solution of CR-C-Dots (fraction 2, 7.5 mg mL^{-1}, 4 mL) and NHS aqueous solution (0.9 mM, 4 mL) were mixed under N_2 atmosphere in a 25 mL three-necked flask followed by addition of 4 mL of EDC aqueous solution (0.9 mM). After vigorous stirring for 20 min, 60 mg of 4-AT dissolved in 5 mL of ultrapure water was added dropwise into the flask in 5 minutes. Then the reaction mixture solutions were adjusted to pH value at 8~9 with sodium hydroxide solution (1 M). Followed by stirring overnight in dark at room temperature, the solution was dialysed for a week in dark against ultra-pure water through a dialysis membrane (MWCO 500-1000 Da).

Characterization

Absorption spectra were carried out on a Varian Cary 300 UV-vis spectrometer and photoluminescence spectra were recorded by a Shimadzu RF-5301PC spectrofluorophotometer. Fluorescence lifetime measurements were conducted on Edinburgh Instruments FLS 920 combined fluorescence lifetime and steady state spectrometer. Lifetime decay curves were fitted into an exponential formula $F(t) = A + B_1 \exp(-t/\tau_1) + B_2 \exp(-t/\tau_2) + B_3 \exp(-t/\tau_3) + B_4 \exp(-t/\tau_4)$ and average

lifetime was calculated according to equation $\tau_{av} = (B_1 \tau_1^2 + B_2 \tau_2^2 + B_3 \tau_3^2 + B_4 \tau_4^2)/(B_1 \tau_1 + B_2 \tau_2 + B_3 \tau_3 + B_4 \tau_4)$. Fourier transform infrared (FT-IR) spectrum was obtained on a NEXUS FT-IR spectrometer (Thermo Nicolet, USA) using KBr pellets. Transmission electron microscope (TEM) measurements were taken on a JEOL JEM-2010HR microscope with an accelerating voltage of 200 KV. Samples for TEM measurements were deposited on an ultrathin carbon film supported by 300-mesh copper grids. X-ray photoelectron spectroscopy (XPS) was performed on a Thermo-VG Scientific ESCALAB 250 spectrometer. Photoelectrons were generated by mono Al Kα X-ray radiation of energy 1486.6 eV and the calibration was based on the C1s with the binding energy at 284.8 eV. Samples for XPS analysis were prepared by depositing aqueous solutions of C-Dots onto a piranha solution and aqua regia-treated silicon wafer and drying in air at room temperature for one day. All spectral peaks were de-convoluted by the XPSPEAK version 4.1 software with the Shirley method for background subtraction and fitted by Gaussian-Lorentzian functions. Confocal microscopy images were obtained with a confocal laser scanning fluorescence microscopy (Zeiss LSM-710, Carl Zeiss, Göttingen, Germany). ESR measurements were carried out using a Bruker EMX A300 spectrometer.

Quantum yields measurements

The quantum yields (QYs) of as-synthesized C-Dots following 360 nm excitation was measured according to the established procedure.[19, 27] Quinine sulfate in 0.1 M H_2SO_4 (QYs 0.54 at 360 nm) was chosen as a standard. In order to minimize reabsorption effects, the absorbance of C-Dots at 360 nm was controlled to be *ca*. 0.05 when using 10 mm fluorescence cuvette.

Cell cytotoxicity tests (MTT)

MTT assay was carried out to evaluate the cytotoxicity of the C-Dots on A549 cell, MCF7 and HeLa cell lines. Cells were cultured in 96-well tissue culture plates (Corning) at a density of 1×10^4 cells per well. After 24 h incubation, the cells were treated with varies concentrations (0.0625, 0.125, 0.25, 0.5, 1 mg mL^{-1}) of the C-Dots. After incubation for 48 h, 20 μL of MTT (5 mg mL^{-1}) was added into each well. The cells were further incubated for 4h, the culture medium was removed and 150 μL of DMSO was added to dissolve the formazan product. The cell viability was evaluated by measuring the absorbance at 490 nm after shaking for 6min.

Cell imaging

A549 cells were cultured at 35 mm dishes for 24 h and cells were incubated with C-Dots (0.5 mg mL^{-1}) for 5 h. Then, the medium was removed and the cells were washed three times with cold PBS. Cellular images were taken by confocal microscopy immediately.

Electron spin resonance (ESR)

ESR measurements were carried out at ambient temperature. 50 μL of sample solutions were put in glass capillary tubes with internal diameters of 1 mm and sealed. The tubes were inserted into the ESR cavity and measured. ESR parameter settings were as follows: microwave frequency 9.87 GHz, modulation amplitude 0.04 G, modulation frequency 100 KHz, scan range 500 G, microwave power 1 mW and time constant 40.96 ms.

Result and discussion

Synthesis, separation and identification of CR-C-Dots and AR-C-Dots

Following pyrolysis of critic acid and bPEI at 200 ^oC for 1h, the resulting reaction mixture was dialysed against pure water to remove small molecule precursor.[28] As illustrated in Scheme 1, when separated and eluted from a Sephadex G25 column, two fractions on the column exhibited strong blue fluorescence while the spacing between them were weakly emitted upon excitation at 365 nm using a hand UV lamp. This allowed easy separation and collection of these two fluorescent fractions, denoted as fraction 1 and 2, respectively (scheme 1). It should be noted that the extremely weakly emitted fraction could also be collected prior to fraction 1, the morphology of which was like viscous oil following evaporation and fit well with the phenotype of unreacted bPEI. The sufficient difference of retention time between bPEI and fraction 1 provided the possibility to remove unreacted bPEI. Low content of ammonia water was necessary to reduce the interaction between amino groups-rich composition and the hydroxyl group of dextrin during chromatography separation. The weight yields of fraction 1 and 2 were 14.6% and 25.2%, respectively, with respect to the contents of citric acid and bPEI. The two highly fluorescent fractions were systematically characterized by TEM, XPS, FT-IR, UV-vis, FL, and fluorescence lifetime decays.

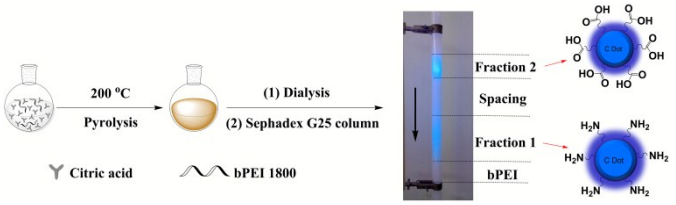

Scheme 1 Schematic representation of one-pot pyrolysis of citric acid and bPEI precursors and separation of formed AR-C-Dots and CR-C-Dots.

TEM characterization indicated that both fractions consisted of small-sized C-Dots, which were near-spherical in morphology and uniformly distributed without any agglomeration (Fig. 1a and b). Their size distribution histograms (inset in Fig. 1a and b) indicated that the average size of fraction 1 was slightly larger than fraction 2 (1.9 nm vs 1.5 nm). This is quite identical to the gel filtration principle that the retention time on the G25 column is mainly determined by the molecular size, larger molecules leaving first followed by smaller ones.

XPS assay was used to characterize the chemical composition of obtained C-Dots. The as-synthesized C-Dots were both composed of carbon, nitrogen and oxygen（Fig. 1c and d）, but more nitrogen contents in fraction 1 and more oxygen in fraction 2. As shown in Fig.1e, the C1s peaks of fraction 1 at 284.1, 284.5, 285.2 and 287.2 eV can be assigned to carbon in the form of C=C (sp^2), C-C (sp^3), C-N (sp^3) and C=O (sp^2), respectively.[24, 29] For the fraction 2, the observed C1s signals at 284.1, 284.5, 286.2, 287.8 and 289.1 eV can be assigned to carbon in the form of C=C (sp^2), C-C (sp^2), C-N (sp^3), C-O-C (sp^3) and O=C-OH, respectively.[24, 30] Quantitative analysis indicated that fraction 1 had less C=C (sp^2) groups, but more C-C (sp^3) and C-N (sp^3) groups than fraction 2, suggesting that more bPEI passivation occurred in fraction 1. Much more C-O-C (sp^3) and O=C-OH groups could be observed in fraction 2, further supporting that fraction 2 was less passivated by bPEI. Much more C-N (sp^3) and low contents of C=O group in fraction 1 might be explained by further reaction of bPEI with C-O-C (sp^3) and O=C-OH groups surrounding the formed carbon core. The slightly bigger size of fraction 1 than 2 might also support the covalent bonding of bPEI onto the surface of carbon core of fraction 1.

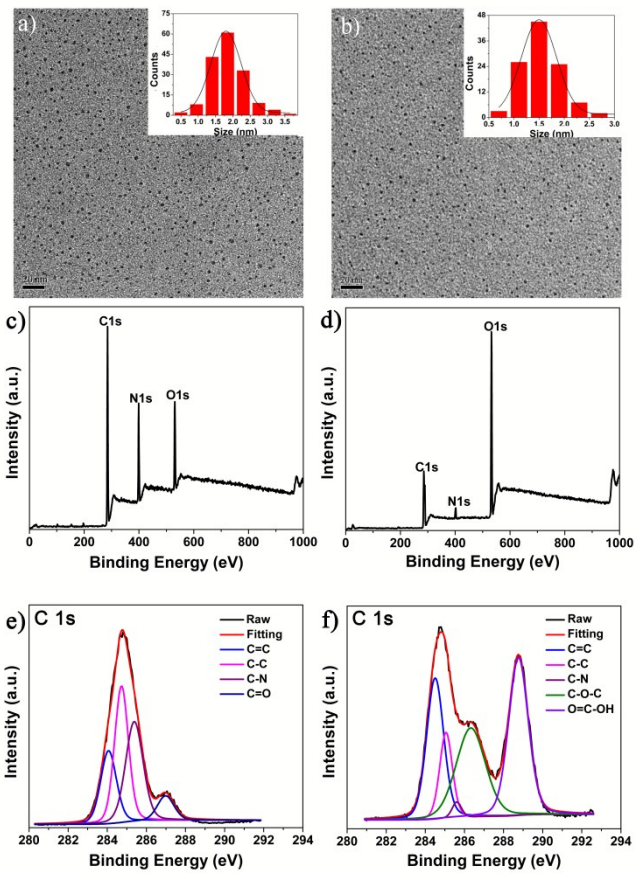

Fig. 1 TEM and XPS characterization of the as-synthesized C-Dots. (a, c, e) for fraction 1 and (b, d, f) for fraction 2. Scale bars in TEM images: 20 nm.

FT-IR spectrum was used to identify the organic functional groups on the surface of the as-synthesized C-Dots. As shown in Fig. 2, the absorbance of fraction 1 at 3404, 2950, 2839, 1577, 1459 and 1297 cm^{-1} was quite similar to bPEI 1800, suggesting that fraction 1 was successfully passivated by bPEI.[31] New peaks at 1644 cm^{-1} can be assigned to C=O stretching vibration of amide group (Amide I) indicating the amide linkage of bPEI in fraction 1.[25] In contrast, the infrared absorbance of fraction 2 was quite different from pure citric acid, bPEI 1800 or fraction 1. A new absorbance peak at 1728 cm^{-1} and broad absorbance at 3130 cm^{-1} was attributed to C=O and OH stretching vibration of carboxyl group, respectively. The strong absorbance at 1400 cm^{-1} can be assigned to in-plain bending vibration of OH group on the surface of fraction 2. Absence of absorbance peaks at 2950 and 2839 cm^{-1} (CH_2 stretching vibration) also suggested fraction 2 wasn't apparently passivated by bPEI.

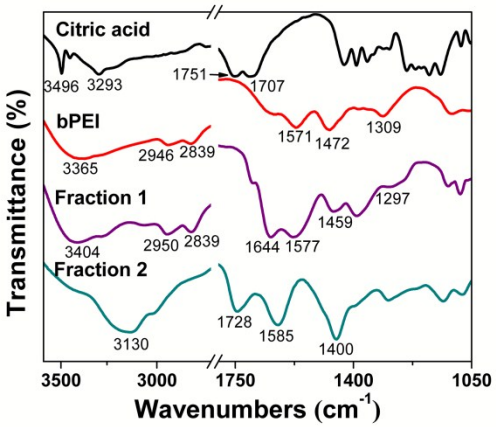

Fig. 2 FT-IR characterization of the as-synthesized C-Dots.

The UV-Vis absorption spectra of fraction 1 and 2 and their photoluminescence (PL) spectrums were shown in Fig. 3a and b, respectively. Both C-Dots exhibited similar absorbance bands centered at 240 nm and 360 nm, attributable to the π-π* transition of nanocarbon and n-π* transition of C=O, similar to previous reports.[24, 32, 33] Interestingly, the emission peak at 445 nm was observed in both emission spectrums of fraction 1 and 2, although nanoparticles in both fractions had different size. This phenomenon further supported that the photoluminescence of C-Dots was not only determined by size.[19] When the excitation wavelength was increased from 360 to 400 nm, the emission peak of both C-Dots didn't shift, implying relatively uniform surface emission trap state.[13, 34] However, the maxima excitation wavelength was slightly different, 370 nm for fraction 1 and 360 nm for fraction 2, respectively, suggesting the as-synthesized C-Dots with different structures. Quantum yields were 8.2% for fraction 1 and 17.4% for fraction 2, quite different from most previous reports that surface passivation enhanced quantum yields of C-Dots.[10, 13, 35] One possible reason was that photoinduced electron transfer (PET) quenching of C-Dots occurred from nitrogen atoms of bPEI to luminescent carbon core in fraction 1, similar to CdSe/ZnS core/shell

quantum dots quenched by nitrogen atoms of surface-linked azamacrocycle.[36]

Fluorescence lifetime measurement indicated that the average decay time was 10.57±0.13 ns for fraction 2, longer than 6.36±0.12 ns for fraction 1, as shown in Fig. 3 and Table S1. The influence of pH and sodium chloride concentration on both kinds of C-Dots was also investigated. As shown in Fig. S1a and b, maximum fluorescence intensity of the fraction 1 was observed at pH 5, whereas fraction 2 showed highest fluorescence intensity at pH 6 (nearly neutral), suggesting different surface groups surrounding the fluorescent C-Dots.[37] Both C-Dots displayed good fluorescence stability in the presence of sodium chloride (even up to 2M) (Fig. S1c and d), implying the potential of as-synthesized C-Dots for cell imaging applications.

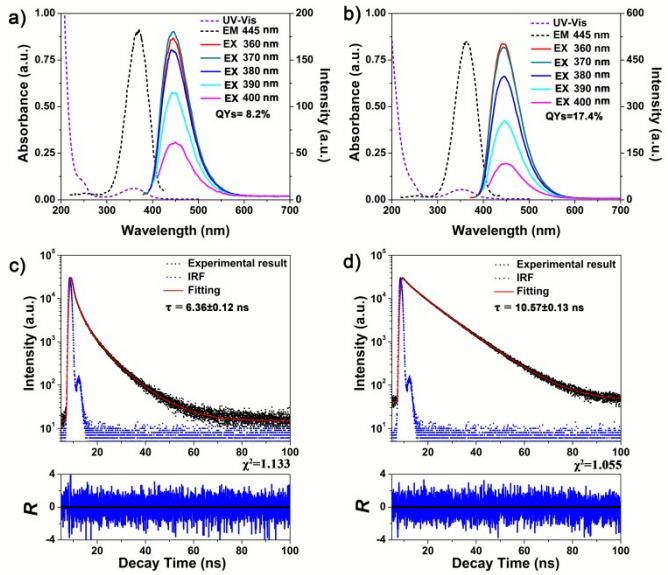

Fig. 3 UV-vis/excitation/emission and fluorescence lifetime characterization of as-synthesized C-Dots. (a, c) for fraction 1 and (b, d) for fraction 2.

The influences of Cu^{2+} and Fe^{3+} on the fluorescence of fraction 1 and fraction 2 were also checked. As shown in Fig. S2, Cu^{2+} quenched the fluorescence of fraction 1 more seriously than Fe^{3+} (K_q of 8.27×10^6 for Cu^{2+} and 2.47×10^6 for Fe^{3+}), which was different from the case of fraction 2 (K_q of 2.44×10^4 for Cu^{2+} and 3.25×10^6 for Fe^{3+}). The result was quite identical to previous reports that Cu^{2+} had a higher thermodynamic affinity and faster chelating process with "N" on the surface of C-Dots, whereas Fe^{3+} exhibited good binding affinity for hydroxyl group surrounding the carbon core.[18, 38] All these results provided solid evidence that AR-C-Dots (fraction 1) and CR-C-Dots (fraction 2) have simultaneously formed during one-pot pyrolysis of citric acid and bPEI precursors, which was not observed in previous research on preparation of bPEI-functionalized C-Dots.[23, 24]

ESR and fluorescence dual-responsive probe for ascorbic acid (AA) based on CR-C-Dots

Due to their excellent photophysical properties, good biocompatibility and rich surface functional group, C-Dots have been used to fabricate sensors for inorganic ions[6, 23, 39, 40] and molecule (glucose,[41] AA[42] and H_2S[43]). Inspired by this, we tried to utilize as-synthesized C-Dots to construct electron spin resonance and fluorescent dual model probe for typical antioxidant AA sensing to further prove the existence of CR-C-Dots. We conjugated as-synthesized CR-C-Dots with paramagnetic nitroxide radical 4-AT through amide condensation, as indicated in Fig. 4a. Through a prolonged time dialysis process (one week), C-Dots-4-AT complexes were obtained, as evidenced by observed ESR signal (triplet peaks), UV-vis absorbance and FT-IR spectroscopy (Fig. S3 and S4). Fig. 4b and c showed the ESR spectrum and fluorescence of C-Dots-4-AT response to AA, respectively. With the addition of AA, the prepared C-Dots-4-AT exhibited the ESR off-on and FL on-off dual-model response to AA at the μM level. The mechanism for ascorbic acid detection has been proposed by Guo *et al.* in Scheme S1.[42] Paramagnetic 4-AT with singly occupied molecular orbital (SOMO) was an electron acceptor. The new non-radiative energy relaxation pathway competed with the fluorescence (FL) process of C-Dots and therefore the C-Dos weakly emitted. Upon addition of AA, paramagnetic 4-AT was reduced to diamagnetic hydroxylamine. The non-radiative electron transfer pathway was blocked and the FL of C-Dots restored. Therefore, existence of CR-C-Dots was further proved.

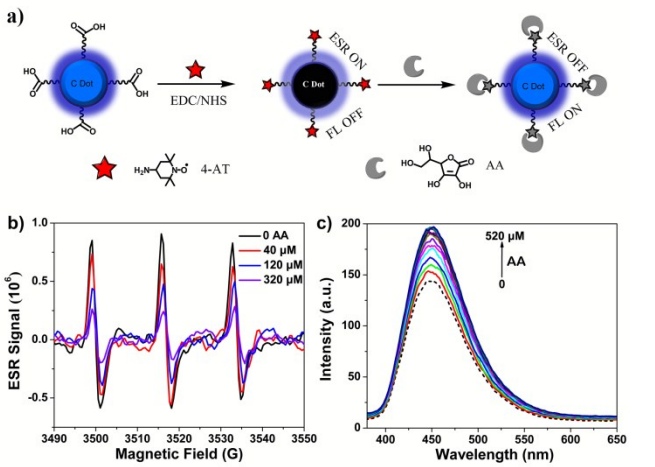

Fig. 4 Construction of ESR and fluorescence dual-responsive probe for ascorbic acid (AA) detection based on CR-C-Dots. (a) Rational design of AA dual-responsive nanoprobe C-Dots-4-AT. (b) and (c) show the ESR signal diminishment and fluorescence enhancement of C-Dots-4-AT upon addition of AA, respectively.

Cell viability and bioimaging application of the obtained C-Dots

The cytotoxicity of AR-C-Dots and CR-C-Dots was evaluated by the MTT assay. Fig. 5a and b showed the viability of three cell lines after incubation with AR-C-Dots and CR-C-Dots at various concentrations for 48 h. The MTT results suggested that the cytotoxicity of two kinds of C-Dots was negligible up to

250 μg mL^{-1}. Owing to their unique PL properties and low cytotoxicity, the potential of the obtained AR-C-Dots and CR-C-Dots for bioimaging was demonstrated on A549 cells. Following incubation with both C-Dots of the same concentration for 5 h, strong fluorescence was observed in the A549 cytoplasm in both cases under confocal laser scanning microscopy (Fig. 5c and d). Control experiments without addition of as-synthesized C-Dots have been carried out to make sure that the autofluorescence from the cells at the same condition has been eliminated (data not shown). It has been found that AR-C-Dots displayed lower quantum yields than CR-C-Dots in solutions, however, slightly stronger fluorescence signals were observed for AR-C-Dots in cell cytoplasm. This indicated easier cellular uptake of AR-C-Dots than CR-C-Dots. This may be due to enhanced interactions between positively-charged AR-C-Dots and cell membrane, also suggesting that AR-C-Dots were rich in amino groups.

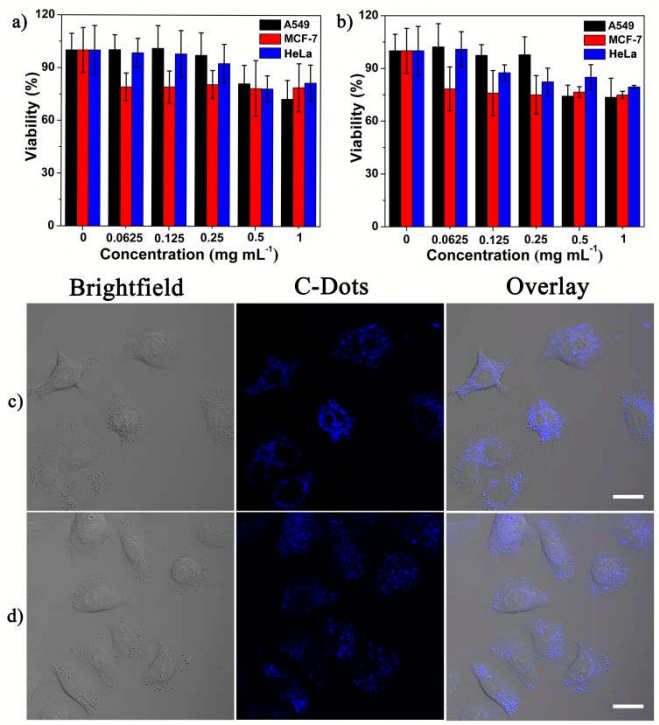

Fig. 5 Cell viability assay and bioimaging applications of the as-synthesized C-Dots. (a, c) for AR-C-Dots and (b, d) for CR-C-Dots. Scale bar: 20 μm.

Conclusions

In this work, co-existence of highly-fluorescent CR-C-Dots and AR-C-Dots during one-pot pyrolysis of citric acid and bPEI precursors was firstly identified. Based on the differences in the size and surface structure, both C-Dots could be easily separated by a Sephadex G25 chromatography. FT-IR spectra and XPS verified the different surface properties of two kinds of C-Dots. CR-C-Dots have a slightly smaller diameter than that of AR-C-Dots (1.5 nm *vs* 1.9 nm). Interestingly, CR-C-Dots had longer fluorescence lifetime and higher quantum yields than AR-C-Dots, quite different from most previous reports that amine group passivation enhanced quantum yields of C-Dots. A fluorescence and ESR dual-responsive nanoprobe for ascorbic acid detection was also constructed to further prove the existence of CR-C-Dots. Preliminary results suggested both C-dots having excellent biocompatibility and great potential for cellular imaging. This work will help understanding the nucleation/surface passivation process during C-Dots formation and facilitate the development of new synthetic/purification strategy for C-Dots.

Acknowledgements

This work was financially supported by the National Natural Science Foundation of China (No. 21231007), 973 Program (No. 2014CB845604), the Ministry of Education of China (Nos. IRT1298 and 313058), Guangdong Provincial Government and the Fundamental Research Funds for the Central Universities.

Notes and references

[a] Department of Applied Chemistry, Institute of Biomaterial, South China Agricultural University, Guangzhou 510642, P. R. China. E-mail: lexyfu@163.com; Fax: +86-20-85287010

[b] School of Chemistry and Chemical Engineering, Sun Yat-Sen University, Guangzhou 510275, P. R. China. E-mail: cesmzw@mail.sysu.edu.cn; Fax: +86-20-84112245

† Electronic Supplementary Information (ESI) available: Figure S1-S4. See DOI:10.1039/b000000x/

1 X. Xu, R. Ray, Y. Gu, H. J. Ploehn, L. Gearheart, K. Raker and W. A. Scrivens, *J. Am. Chem. Soc.*, 2004, **126**, 12736-12737.

2 S. N. Baker and G. A. Baker, *Angew. Chem. Int. Ed.*, 2010, **49**, 6726-6744.

3 H. T. Li, Z. H. Kang, Y. Liu and S. T. Lee, *J. Mater. Chem.*, 2012, **22**, 24230-24253.

4 L. Cao, X. Wang, M. J. Meziani, F. Lu, H. Wang, P. G. Luo, Y. Lin, B. A. Harruff, L. M. Veca, D. Murray, S.-Y. Xie and Y.-P. Sun, *J. Am. Chem. Soc.*, 2007, **129**, 11318-11319.

5 S.-T. Yang, L. Cao, P. G. Luo, F. Lu, X. Wang, H. Wang, M. J. Meziani, Y. Liu, G. Qi and Y.-P. Sun, *J. Am. Chem. Soc.*, 2009, **131**, 11308-11309.

6 W. Shi, X. Li and H. Ma, *Angew. Chem. Int. Ed.*, 2012, **51**, 6432-6435.

7 A. Zhu, Q. Qu, X. Shao, B. Kong and Y. Tian, *Angew. Chem. Int. Ed.*, 2012, **51**, 7185-7189.

8 L. Cao, S. Sahu, P. Anilkumar, C. E. Bunker, J. Xu, K. A. S. Fernando, P. Wang, E. A. Guliants, K. N. Tackett and Y.-P. Sun, *J. Am. Chem. Soc.*, 2011, **133**, 4754-4757.

9 H. Choi, S.-J. Ko, Y. Choi, P. Joo, T. Kim, B. R. Lee, J.-W. Jung, H. J. Choi, M. Cha, J.-R. Jeong, I.-W. Hwang, M. H. Song, B.-S. Kim and J. Y. Kim, *Nat Photon*, 2013, **7**, 732-738.

10 P. Huang, J. Lin, X. Wang, Z. Wang, C. Zhang, M. He, K. Wang, F. Chen, Z. Li, G. Shen, D. Cui and X. Chen, *Adv. Mater.*, 2012, **24**, 5104-5110.

11 M. Zheng, S. Liu, J. Li, D. Qu, H. Zhao, X. Guan, X. Hu, Z. Xie, X. Jing and Z. Sun, *Adv. Mater.*, 2014, **26**, 3554-3560.

12 Y. Choi, S. Kim, M.-H. Choi, S.-R. Ryoo, J. Park, D.-H. Min and B.-S. Kim, *Adv. Funct. Mater.*, 2014, **24**, 5781-5789.

13 Y.-P. Sun, B. Zhou, Y. Lin, W. Wang, K. A. S. Fernando, P. Pathak, M. J. Meziani, B. A. Harruff, X. Wang, H. Wang, P. G. Luo, H. Yang,

M. E. Kose, B. Chen, L. M. Veca and S.-Y. Xie, *J. Am. Chem. Soc.*, 2006, **128**, 7756-7757.
14 L. Bao, Z.-L. Zhang, Z.-Q. Tian, L. Zhang, C. Liu, Y. Lin, B. Qi and D.-W. Pang, *Adv. Mater.*, 2011, **23**, 5801-5806.
15 A. B. Bourlinos, R. Zbořil, J. Petr, A. Bakandritsos, M. Krysmann and E. P. Giannelis, *Chem. Mater.*, 2012, **24**, 6-8.
16 A. B. Bourlinos, M. A. Karakassides, A. Kouloumpis, D. Gournis, A. Bakandritsos, I. Papagiannouli, P. Aloukos, S. Couris, K. Hola, R. Zboril, M. Krysmann and E. P. Giannelis, *Carbon*, 2013, **61**, 640-643.
17 H. Zhu, X. Wang, Y. Li, Z. Wang, F. Yang and X. Yang, *Chem. Commun.*, 2009, 5118-5120.
18 S. Zhu, Q. Meng, L. Wang, J. Zhang, Y. Song, H. Jin, K. Zhang, H. Sun, H. Wang and B. Yang, *Angew. Chem. Int. Ed.*, 2013, **52**, 3953-3957.
19 S. Hu, A. Trinchi, P. Atkin and I. Cole, *Angew. Chem. Int. Ed.*, 2015, **54**, 2970-2974.
20 D. Qu, M. Zheng, L. Zhang, H. Zhao, Z. Xie, X. Jing, R. E. Haddad, H. Fan and Z. Sun, *Sci. Rep.*, 2014, **4**.
21 C. Ding, A. Zhu and Y. Tian, *Acc. Chem. Res.*, 2013, **47**, 20-30.
22 X. Li, S. Zhang, S. A. Kulinich, Y. Liu and H. Zeng, *Sci. Rep.*, 2014, **4**.
23 Y. Dong, R. Wang, G. Li, C. Chen, Y. Chi and G. Chen, *Anal. Chem.*, 2012, **84**, 6220-6224.
24 Y. Dong, R. Wang, H. Li, J. Shao, Y. Chi, X. Lin and G. Chen, *Carbon*, 2012, **50**, 2810-2815.
25 C. Liu, P. Zhang, X. Zhai, F. Tian, W. Li, J. Yang, Y. Liu, H. Wang, W. Wang and W. Liu, *Biomaterials*, 2012, **33**, 3604-3613.
26 J. C. Vinci, I. M. Ferrer, S. J. Seedhouse, A. K. Bourdon, J. M. Reynard, B. A. Foster, F. V. Bright and L. A. Colon, *J. Phys. Chem. Lett.*, 2013, **4**, 239-243.
27 A. M. Brouwer, *Pure Appl. Chem.*, 2011, **83**, 2213-2228.
28 M. J. Krysmann, A. Kelarakis, P. Dallas and E. P. Giannelis, *J. Am. Chem. Soc.*, 2012, **134**, 747-750.
29 K. Linehan and H. Doyle, *J. Mater. Chem. C*, 2014, **2**, 6025-6031.
30 Y. Hu, J. Yang, J. Tian, L. Jia and J.-S. Yu, *Carbon*, 2014, **77**, 775-782.
31 L. Shen, L. Zhang, M. Chen, X. Chen and J. Wang, *Carbon*, 2013, **55**, 343-349.
32 A. Jaiswal, S. S. Ghosh and A. Chattopadhyay, *Chem. Commun.*, 2012, **48**, 407-409.
33 W. Liu, *Chem. Commun.*, 2012, **48**, 7955-7957.
34 Y. Liu, N. Xiao, N. Gong, H. Wang, X. Shi, W. Gu and L. Ye, *Carbon*, 2014, **68**, 258-264.
35 C. J. Liu, P. Zhang, F. Tian, W. C. Li, F. Li and W. G. Liu, *J. Mater. Chem.*, 2011, **21**, 13163-13167.
36 M. J. Ruedas-Rama and E. A. H. Hall, *Anal. Chem.*, 2008, **80**, 8260-8268.
37 S. H. Jin, D. H. Kim, G. H. Jun, S. H. Hong and S. Jeon, *ACS Nano*, 2012, **7**, 1239-1245.
38 A. Zhao, C. Zhao, M. Li, J. Ren and X. Qu, *Anal. Chim. Acta*, 2014, **809**, 128-133.
39 H. X. Zhao, L. Q. Liu, Z. D. Liu, Y. Wang, X. J. Zhao and C. Z. Huang, *Chem. Commun.*, 2011, **47**, 2604-2606.
40 J.-M. Liu, L.-p. Lin, X.-X. Wang, L. Jiao, M.-L. Cui, S.-L. Jiang, W.-L. Cai, L.-H. Zhang and Z.-Y. Zheng, *Analyst*, 2013, **138**, 278-283.
41 W. B. Shi, Q. L. Wang, Y. J. Long, Z. L. Cheng, S. H. Chen, H. Z. Zheng and Y. M. Huang, *Chem. Commun.*, 2011, **47**, 6695-6697.
42 F. Lin, D. Pei, W. He, Z. Huang, Y. Huang and X. Guo, *J. Mater. Chem.*, 2012, **22**, 11801-11807.
43 C. Yu, X. Li, F. Zeng, F. Zheng and S. Wu, *Chem. Commun.*, 2013, **49**, 403-405.